QUANTITATIVE RADIATION MEASUREMENTS OF THE PULSED PLASMA MICROTHRUSTER

Tomokazu Umeki* and Peter J. Turchi†
The Ohio State University
Columbus, Ohio, USA

Abstract

Absolute spectral-radiance of the emission spectra from the exhaust of a Pulsed Plasma Microthruster (PPT) was spectroscopically obtained with an intensified charged-coupled-devise (ICCD) detector, a spectral-radiance calibration lamp and other related optics. The measured values of spectral radiance are used to evaluate the electromagnetic effect of the PPT exhaust to sensitive equipment such as optical sensors carried by a satellite. The benchmark PPT was operated at 10 J energy level for quantitative spectroscopy. Species in the spectra range of 400 to 700 nm were identified followed by measurements of the absolute amount of the spectral radiance for each spectrum. The possible sources of electromagnetic disturbance from the PPT exhaust to the optical sensor were singly and doubly ionized carbon species ranging from 3280 to 520 μW/(sr-mm^2-nm) of spectral radiance.

Introduction

The Pulsed Plasma Microthruster (PPT) has been a very practical device for satellite orbit position control due to its fine thrust-adjust capability as well as structural simplicity and robustness despite of low efficiency. [1] Electromagnetic Interference (EMI) from the PPT exhaust can be significantly adverse to sensitive equipment on-board (e.g optical sensors carried by Space Technology 3 Mission satellites) and must be investigated in advance. The present paper evaluates such possible effects by disclosing the emission sources and their absolute amounts of spectral radiance after conducting quantitative spectroscopic measurements of the electromagnetic radiation from the PPT exhaust.

Experimental Apparatus

The quantitative spectroscopic measurements were performed at The Ohio State University Aeronautical & Astronautical Research Laboratory (OSUAARL) with the following apparatus:

Vacuum Facility

A 1.3 m^3 stainless-steel vacuum tank has a cylinder-shape (0.6m dia x 4.8 m length). Pressure inside the tank was measured with Varian 531 Thermocouple Gauge Tube with 801 Thermocouple Gauge Controller (0.001 to 2 Torr range). It is kept at 3 milliTorr with two vacuum pumps (Welch 1374 DuoSeal Vacuum Pump ; ultimate pressure = 0.1 milliTorr). Each pump is connected to the one end of the tank.

PPT Thruster

The benchmark PPT [2] built at OSUAARL was used for the measurement. It consists of a thrust chamber and an LRC circuitry. The chamber is constructed with two copper electrodes and a Teflon propellant. The width of the electrode and the gap between two electrodes are 2.54 cm. The Teflon was originally positioned 2.54 cm from the tip of the electrodes. The LRC circuitry consists of a 116 nH external inductance, a 16 mΩ external resistance and a 10 μF storage capacitance.

Spectroscopic System

The spectroscopic system, shown in Fig.1 and Fig.2, comprises a condensing lens, a

---

*Graduate Research Assistant
†Professor

spectrometer, a detector, a Geissler tube, a HeNe laser, and a spectral-radiance calibration lamp .

The condensing lens (f/=5, focal length = 25 cm) with an iris images the optical object onto the entrance slit (set to 50 μm) of the spectrometer. For this measurement, all data were obtained in side-on direction 2.54 cm from the electrodes exit plane above the center of the electrodes assuming that the optical sensor is located on one side of the thruster.

The spectrometer (RTS Laboratory) has a focal length 1.2 m with f/=10 and carries a 1200 grooves/mm grating (Bausch & Lomb) yielding the reciprocal linear dispersion of ~0.6 nm/mm (for the first order spectra) at the exit slit. The light dispersed by this grating is focused onto the intensified charged-coupled-device (ICCD) camera detector (Princeton Instruments 576S/RB-E). The ICCD detector has 576 x 384 pixel format (12.7 X 8.5 mm) and 50 ns minimum gating. These features enable to obtain spatially and temporally resolved spectroscopic data. It has also 16 bits dynamic range with variable gain for sensitivities 1 to 100 counts per photoelectron to detect very low-intensity light. Spectral range of the ICCD camera is 180 ~ 800 nm. The spectral resolution for the first order spectra on the ICCD detector is 0.013 nm/pixel changing slightly with the wavelength.

Geissler tubes (Sargent-Welch Scientific Company, Edmund Scientific Company) were used to calculate the wavelengths of observed spectra. These include argon, chlorine gas, helium, mercury vapor, neon, and xenon tubes.

A HeNe laser (Melles Griot, 0.5 mW) was used for obtaining optical alignment by guiding its beam from the spectrometer exit-slit to the entrance slit and thereby locating the position of the optical object.

An absolute spectral-radiance calibration lamp (The Eppley Laboratory) was used to obtain the absolute value of spectral radiance in μW/(sr-mm^2-nm) from the ICCD-detector output in count. This conversion process is explained later. The lamp is calibrated for the range of 225 to 2400 nm and has a tungsten ribbon filament 10 cm behind a fused silica window 3 cm in diameter through which the radiation was measured.

Diagnostics and Results

Current Waveform

PPT was operated for 10 J energy level. The current waveform was computed numerically as shown in Fig.3 by integrating I-dot (current value derivative with respect to time) signal obtained from the Rogowski coil[2].
As seen in the figure, the entire event of thrusting ends in 15 μs. This value was used later to determine the gate width or shutter period of the ICCD detector.

Species Identification

Emission spectra were measured from 400 to 700 nm in this work to disclose the light-source species in the electromagnetic radiation from the PPT exhaust.

The gate or the shutter of the ICCD detector was opened 0.1 μs
after triggered by the signal from the Rogowski coil at the PPT ignition. Then the gate was kept opened for 15 μs to capture the whole event of the radiation. The intensifier gain was set to 40. Data acquisition was repeated at least seven times to observe the reasonable repeatability by checking if there is no outstanding output-variation between each time of the acquisition. The typical variation was ± 10 to15 %.

The wavelength of an observed spectrum was calculated by interpolating
or extrapolating the known wavelengths[3] of spectra from the Geissler tubes. One example of the observed spectrum from the PPT exhaust is shown in Fig. 4. along with the Geissler-tube spectra used for the wavelength calculation. The Geissler-tube spectra in this figure are argon lines of 425.1185, 425.9362, 426.6286, 427.2169, and 430.010 nm, respectively.[3] Interpolating 426.6286 and 427.2169 nm, the wavelength of the spectrum from the PPT exhaust was obtained. As seen from the figure, the wavelength-range that one data acquisition can cover is about 8nm depending on the wavelength.

This procedure was repeated to cover the range of 400 to 700 nm. The resulted spectra are shown in Fig.5 with the identified species which were determined by the existence of a set of spectral lines of known wavelength[3], [4] of the species. The most of the observed spectra other than singly ionized carbon, doubly ionized carbon and neutral hydrogen in the figure were singly

ionized nitrogen and singly ionized oxygen.

Absolute Spectral-radiance Measurement

As the first step to convert the ICCD output in count to the absolute spectral-radiance in μW/(sr-mm^2-nm), the radiation from the spectral-radiance lamp was measured with the ICCD detector. The measurement was performed at each wavelength of the observed species since the ICCD detector sensitivity varies along the wavelength.

The lamp was set to the position where the PPT was located and the tungsten filament was focused onto the entrance slit of the spectrometer with the same condensing lens. The lamp was operated at 35 A since the lamp was calibrated at 35 A to provide the reference spectral-radiance values. The setting of the ICCD detector was exactly same as the case of PPT-exhaust measurements except that the gate of the ICCD detector was opened by the signal from a waveform generator (Wavetek 50MHz Pulse/Function Generator) in stead of the Rogowski signal and the gate opening-width was set to 1 ms in stead of 15 μs. 15 μs of gating did not provide enough exposure to the detector from the lamp and 1 ms of gating yielded the same order of magnitude of the output in count compared to the case of PPT-exhaust measurements. Hence the value of spectral-radiance needs to be multiplied by 1 ms / 15 μs to compensate this difference in exposure time when the detector outputs from the PPT exhaust are compared to those from the lamp.

The correlation between the ICCD output and the spectral-radiance after the time compensation (namely, the spectral-radiance values multiplied by 1 ms / 15 μs) is graphed in Fig. 6. Between data points, values are interpolated. Using this correlation, the conversion factor from the ICCD output to the spectral radiance is obtained along the wavelength of interest by simply dividing the spectral-radiance value by the ICCD-output value of the same wavelength. The resulted conversion-factor values in μW/(sr-mm^2-nm)/count is shown in Fig.7. Based on this conversion factor, the observed spectra in count in Fig.5 can now be expressed in absolute spectral-radiance in μW/(sr-mm^2-nm) as shown in Fig.8.

Conclusions and Discussions

The emission sources from the 10J PPT exhaust and their absolute amounts of spectral radiance were obtained from quantitative spectroscopy to evaluate the electromagnetic disturbance to the optical sensor. In 400 to 700 nm range, the most potential sources of disturbance and their absolute values of spectral radiance are 426.7 nm CII (3280 μW/(sr-mm^2-nm) max), 464.7 nm CIII (1460 μW/(sr-mm^2-nm) max) , 465.0 nm CIII (1120 μW/(sr-mm^2-nm) max) , 657.8 nm CII (920 μW/(sr-mm^2-nm) max) and 658.3 nm CII (520 μW/(sr-mm^2-nm) max).

These results may be dependant on the operating conditions and environment such as energy level, thrust frequency, background pressure and electrode material. Background pressure effects due to contaminants such as hydrogen, nitrogen, and oxygen are isolated as the main factors for such dependancy. UV range spectra normally considered to be strong energy sources were not examined since they can be easily circumvented by proper placement of a protective plate between the thruster and the sensitive equipment. Indeed, during our experiment emission below 350 nm was blocked by the plexiglass optical-window attached to the vacuum tank.

Although singly-ionized-carbon lines of strong intensity were observed, no outstanding singly-ionized-fluorine line was observed. This seems to be due to the very low values of the product of the transition probability and the density of the fluorine emitter in the upper excited state (more precisely it is the integration value of the density across the line of sight). Knowing that some fluorine lines have the transition probabilities of the same order of magnitude as those of observed carbon lines, the emitter density considered to be very low. In fact, some of singly-ionized-carbon lines which have the same order transition-probability were not observed. This should be due to the same reason. On the other hand, neutral-hydrogen lines of high spectral radiance were clearly observed due to the large value of the transition probabilities.

These spectral radiance measurements can be utilized to calculate the amount of electromagnetic radiation from the PPT exhaust. This can be accomplished by obtaining radiance values with respect to spectral width and

considering the appropriate solid angle and area, and the emitting time period. This analysis will allow the evaluation of radiative energy losses and thus quantify their contribution to the thruster's efficiency degradation.

Acknowledgments

The authors would like to thank Eric Pencil at NASA Glenn Research Center and Henry Baust at Wright-Patterson Air Force Base for allowing us to use some of their optical equipment. This work was supported by NASA Glenn Research Center under NAG3-843.

References

[1] Myers, R.M., "Electromagnetic Propulsion for Spacecraft", AIAA 93-1086, Feb. 1993
[2] Kamhawi, H., Turchi, P.J., Leiweke, R.J., and Myers, R.M., "Design and Operation of A Laboratory Benchmark PPT", AIAA 96-2732, July 1996.
[3] Weast, R.C., *CRC Handbook of Chemistry and Physics,* CRC Press. Inc., Boca Raton, Florida, 1984.
[4] Wiese, W.L., Smith, M.W., and Glennon, B.M., *Atomic Transition Probabilities,* National Bureau of Standards, May 1966.

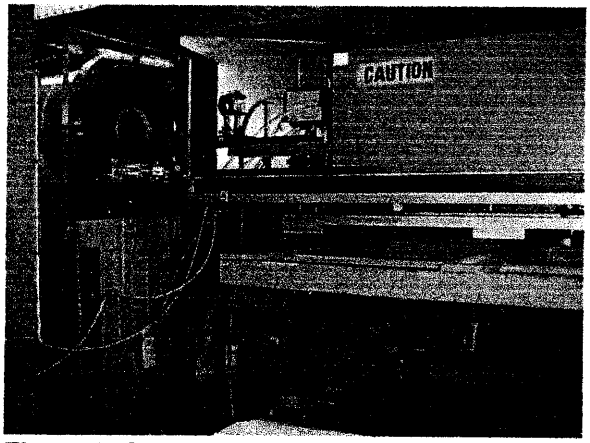

Figure 1. Overview of the spectroscopic system

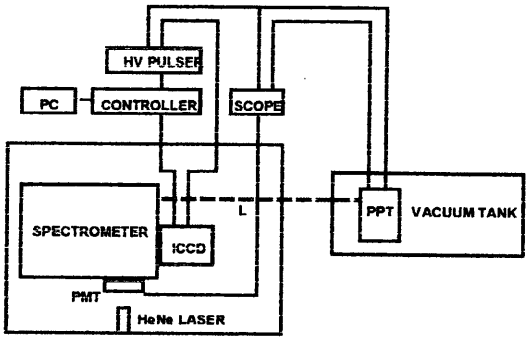

Figure 2. Schematic of the spectroscopic system

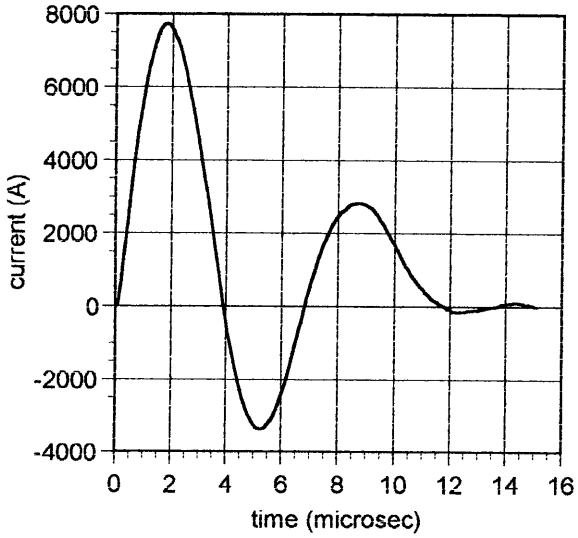

Figure 3. Current waveform

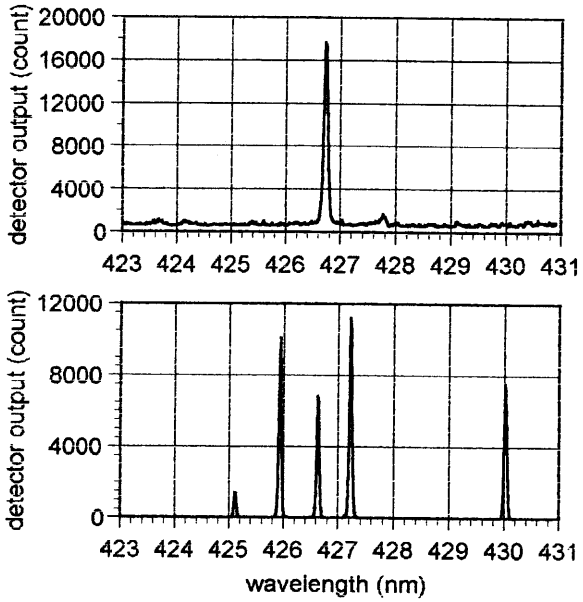

Figure 4. Observed spectrum for the PPT exhaust and Geissler-tube spectra.

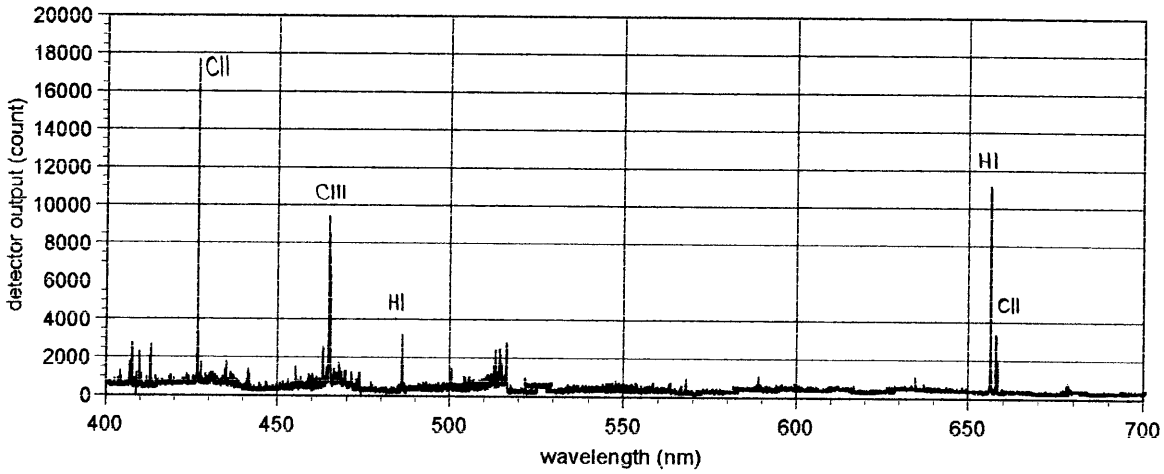

Figure 5. Observed spectra from 400 to 700nm with identified species

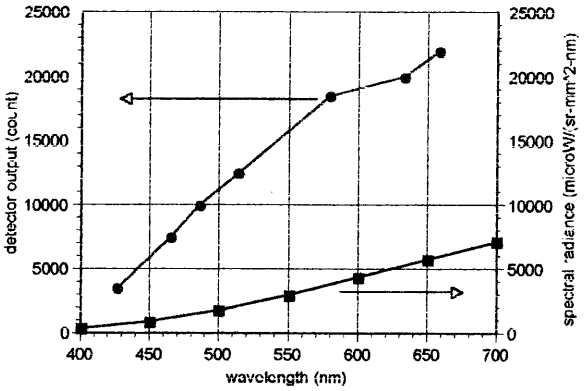

Figure 6. The correlation between the spectral radiance and the detector output.

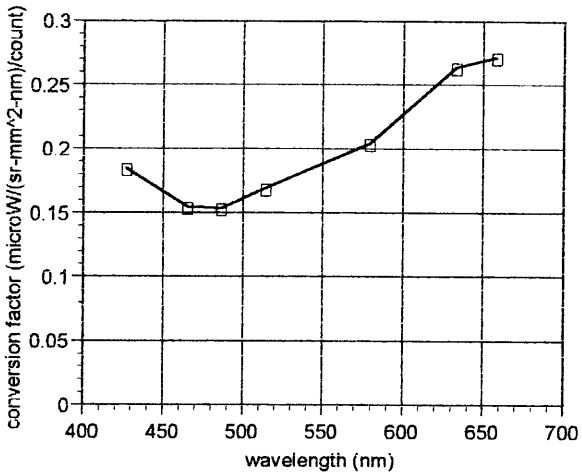

Figure 7. The conversion factor from the detector output to the spctral radiance.

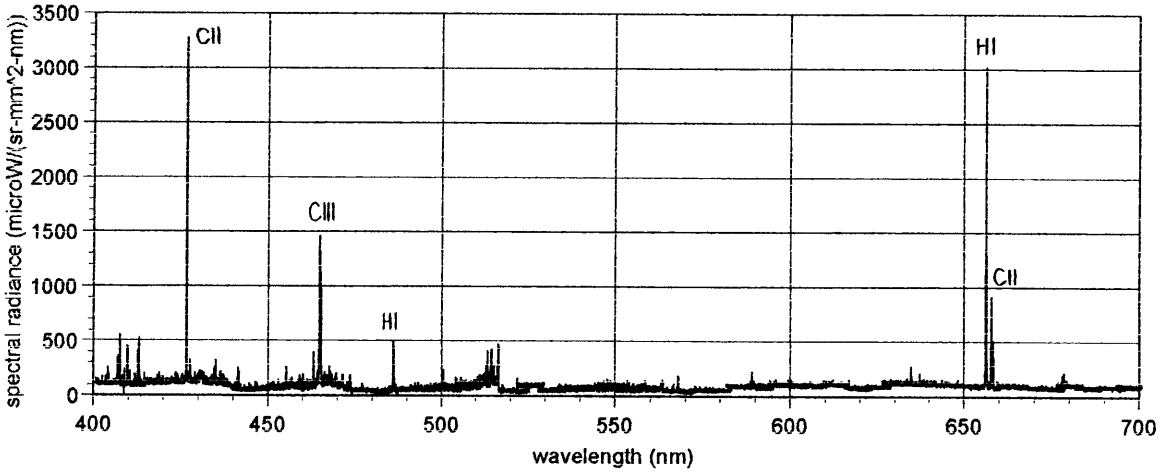

Figure 8. The absolute spectral radiance of the observed spectra.